The beneficial effects of molybdenum addition on Ni–B amorphous alloy catalyst used in 2-ethylanthraquinone hydrogenation

YONGJIANG HOU*
Key Laboratory of Contaminant Control in Biology of Hebei Province, College of Environmental Science and Engineering, Hebei University of Science and Technology, Shijiazhuang 050018, Hebei Province, P.R. China
E-mail: hyj@hebust.edu.cn

YAQUAN WANG, ZHENTAO MI
Schools of Chemical Engineering and Technology, Tianjin University, Tianjin 300072, P.R. China

Published online: 1 November 2005

Amorphous alloys, since first being used as catalyst by Smith [1] in 1980, have found many applications in the field of catalysis due to their special characteristics: short-term order and long-term disorder. Among them, Ni–B amorphous alloy prepared by chemical reduction method exhibits more advantages than others owing to its convenient preparation and unique selectivity in many hydrogenation processes [2–10], not to mention its relatively lower cost corresponding to the cost of precious metals, which are usually used as hydrogenation catalysts. In addition, compared with Raney Ni, another conventional hydrogenation catalyst, almost no pollutant is released during the preparation of Ni–B amorphous alloy [2]. However, both the activity and the thermal stability of Ni–B amorphous alloy have to be enhanced in order to find applications in industries [7]. In our previous works [9, 10], we found that the thermal stability of the catalyst was not enhanced despite the increase in the activities with La and Ce additions. In the present paper, a series of Mo-doped Ni–B amorphous alloy catalysts were prepared by the method of potassium borohydride (KBH_4) reduction and evaluated in the reaction of 2-ethylanthraquinone (EAQ) hydrogenation. This reaction was mainly used to produce hydrogen peroxide through anthraquinone route [11]. The promoting effects of Mo on both the catalytic activity and the thermal stability of the amorphous alloy were studied based on the catalysts evaluation and the analyses, using Differential Scanning Calorimeter (DSC), X-ray Diffraction (XRD), X-ray photoelectron spectroscopy (XPS), and so on.

The Ni–B amorphous alloy was prepared by the usual method of KBH_4 reduction, detailed procedure was shown in our previous reports [10]. The Mo-doped Ni–B amorphous alloy was prepared by the same procedure in which the calculated amounts of $(NH_4)_6Mo_7O_{24}{\cdot}4H_2O$ were added into the $NiCl_2$ aqueous solution. The heating treatment of the samples was carried out at elevated temperatures (300 and 500 °C) in ultrahigh purity H_2 flow for 2 hr.

The composition of catalysts was measured by an inductively coupled plasma (ICP) instrument. DSC was conducted under pure nitrogen atmosphere on a SHIMADZU TA-50 system to study the effects of Mo on the thermal stability of Ni–B amorphous alloy. The amorphous and crystalline characters of the as-prepared alloys were verified by XRD executed on a Rigaku D/max-2500 powder diffractometer with Cu Kα radiation (40 kV, 100 mA). XPS analysis was carried out on a PHI 1600 ESCA system by using a Mg Kα radiation (1253.6 eV) at a base pressure of 1×10^{-8} Torr to study the surface elemental states of the catalysts. H_2-chemisorption and H_2 temperature programmed desorption (H_2-TPD) were performed by using a MICROMETRITICS ASAP 2910 instrument so as to obtain the information of the H_2 adsorption and desorption on the surface of the catalysts. All catalysts were evaluated by the hydrogenation of 2-ethylanthraquinone (EAQ), which was specifically described in our previous work [10]. The catalyst activity was expressed as the amount of hydrogen peroxide produced per gram catalyst per minute ($g_{H_2O_2}\ g_{cat}^{-1}\ min^{-1}$).

The results of BET areas, compositions, and H_2-chemisorption of various catalysts are listed in Table I. In order to facilitate the following discussions, the compositions of B and Mo are expressed as atomic ratios to Ni. In the case of BET area, it is increased with the increase of the Mo contents, indicating Mo might has a dispersing effect, resulting in higher BET areas. With respect to the H_2-chemisorption, the values first increase and then decrease along with the increase of the Mo contents. Theoretically, there are two factors that influence the amounts of H_2 chemical adsorption on Ni surface while discussing the effects of dopants: structural effect and electronic effect [12]. XPS analysis demonstrates that there is no obvious difference in the B_{1s} and $Ni_{2p3/2}$ XPS spectra after Mo addition, implying that the electronic effect of Mo on the obtained catalysts could be neglected. Therefore, the main factor affecting H_2 adsorption here is the structure effect of Mo dopant. With this consideration, the aforementioned tendency about the H_2-chemisorption indicates that Mo might effectively disperse the catalysts, presenting more surface Ni atoms, thus leading to more

* Author to whom all correspondence should be addressed.

0022-2461
DOI: 10.1007/s10853-005-4223-6

TABLE I The properties and activities of the obtained catalysts

Sample[a]	BET area ($m^2\ g_{cat}^{-1}$)	H_2-chemisorption ($cm^3\ g_{cat}^{-1}$) (STP)	EAQ hydrogenation activity ($\times 10^3\ g_{H_2O_2}\ g_{cat}^{-1}\ min^{-1}$)
$Ni_1B_{0.645}$	12.8	0.59	1.2
$Ni_1B_{0.667}Mo_{0.014}$	28.5	0.78	2.7
$Ni_1B_{0.685}Mo_{0.020}$	42.1	1.31	3.7
$Ni_1B_{0.735}Mo_{0.025}$	48.4	2.45	6.9
$Ni_1B_{0.757}Mo_{0.034}$	62.0	1.26	1.7
$Ni_1B_{0.735}Mo_{0.025}$[b]	11.2	0.21	0.2
$Ni_1B_{0.735}Mo_{0.025}$[c]	4.1	0.1	0.1

[a]The numbers in this column denote the atomic ratios of B and Mo to Ni determined by ICP.
[b]The sample treated at 573 K for 2 hr under H_2 flow.
[c]The sample treated at 773 K for 2 hr under H_2 flow.

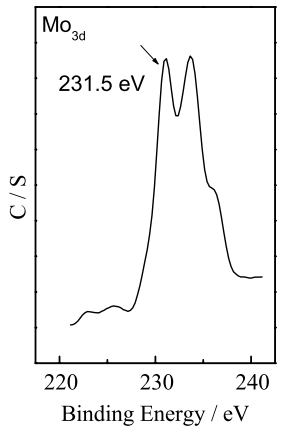

Figure 1 $Mo_{3d5/2}$ XPS spectra of $Ni_1B_{0.735}Mo_{0.025}$.

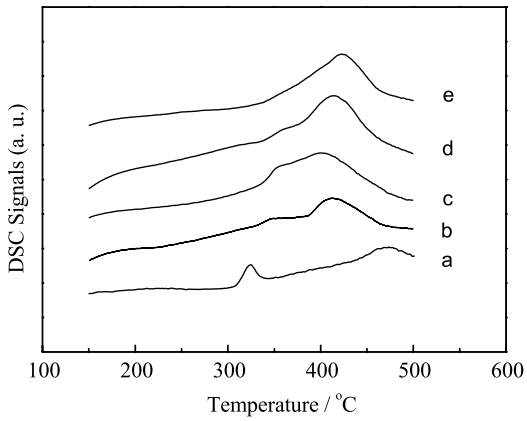

Figure 2 DSC spectra of Mo-doped Ni–B amorphous alloy catalysts: (a) $Ni_1B_{0.645}$, (b) $Ni_1B_{0.667}Mo_{0.014}$, (c) $Ni_1B_{0.685}Mo_{0.020}$, (d) $Ni_1B_{0.735}Mo_{0.025}$, (e) $Ni_1B_{0.757}Mo_{0.034}$.

hydrogen adsorbed. However, overmuch Mo species might detrimentally cover some surface Ni atoms, resulting in less hydrogen being adsorbed.

Fig. 1 shows the $Mo_{3d5/2}$ XPS spectra of the $Ni_1B_{0.735}Mo_{0.025}$ amorphous alloy catalyst. The peak of $Mo_{3d5/2}$ electron-binding energy was found to be at 231.5 eV, indicating that Mo existed as Mo^{6+} species on the surface of the catalysts. This phenomenon was observed by Chen *et al.* [13] during the preparation of Mo-doped Co–B amorphous alloy which was attributed by them to the fact that Mo^{6+} species were not reduced by KBH_4 during the preparation. However, the real state of Mo dopant in the alloyed catalysts is still unclear only with surface analysis because Mo is prone to oxidation to Mo^{6+}. This needs to be studied further with other analyses.

Unacceptable thermal stability of Ni–B amorphous alloy produced by chemical reduction is an important factor restricting its industrial application. Thus, the effect of Mo on the thermal stability was studied first with DSC instrument. Fig. 2 shows the DSC spectra of Ni–B and Mo-doped Ni–B catalysts. For $Ni_1B_{0.645}$ catalyst, it is found that there are two exothermic peaks: one around 320 °C and the other around 470 °C, indicating two crystallization processes. According to other report [14], the two exothermic peaks could be assigned to the formation of Ni_3B and Ni_2B crystalline phases, and the transformation of Ni_3B and Ni_2B crystalline phases to Ni crystalline clusters. From the viewpoint of amorphous alloy, the first peak might be suitable to denote the thermal stability of the obtained samples because the amorphous structure disappears after that. With the addition of Mo, it is found that the first peak shifts to higher temperature, the second peak shifts to lower temperature, and finally both of them overlap with only one peak around 420 °C, indicating that the crystallization processes of Ni–B amorphous alloy are altered and the thermal stability of the amorphous alloy is strengthened. Walter [15] has reported that the addition of some bigger atom in FeB amorphous alloy results in higher crystallization temperature owing to the structure effect of the dopant which prevents the gathering of Fe atoms. Therefore, in the present work, the reason also might be attributed to the structure effect of Mo, preventing the gathering of the Ni atom, resulting in higher crystallization temperature.

In order to study further the effect of Mo on thermal stability, XRD analyses of $Ni_1B_{0.645}$ and $Ni_1B_{0.735}Mo_{0.025}$ catalysts with and without heat treatment were carried out as shown in Fig. 3. Without the heat treatment, it is found that for both of them there is only one broad peak around $2\theta = 45°$, characteristic of a typical amorphous structure [16]. After heating them at 300 °C for 2 hr, some peaks appear in the XRD spectrum of $Ni_1B_{0.645}$ catalyst, indicating the formation of Ni_3B and Ni_2B crystalline phases [14], while only some small Ni crystalline diffraction peaks appear in the XRD spectrum of $Ni_1B_{0.735}Mo_{0.025}$, meaning that the first crystallization process is altered and no Ni_3B and Ni_2B crystalline phases are formed with the addition of the Mo. After heat treatment at 500 °C for about

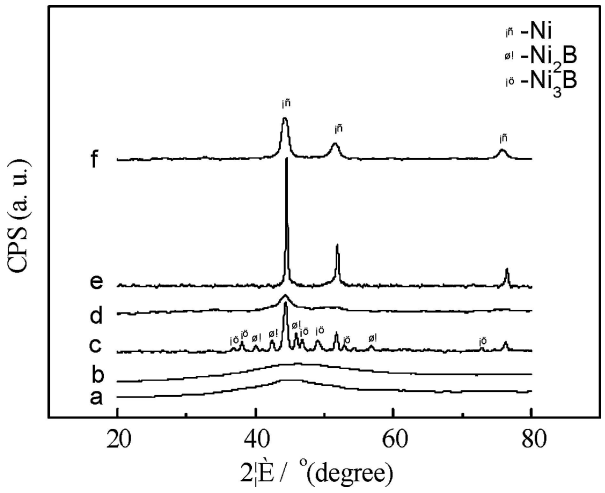

Figure 3 XRD spectra of $Ni_1B_{0.645}$ and $Ni_1B_{0.735}Mo_{0.025}$ treated at different temperatures: (a) $Ni_1B_{0.645}$, (b) $Ni_1B_{0.735}Mo_{0.025}$, (c) $Ni_1B_{0.645}$ treated at 300 °C for 2 hr, (d) $Ni_1B_{0.735}Mo_{0.025}$ treated at 300 °C for 2 hr, (e) $Ni_1B_{0.645}$ treated at 500 °C for 2 hr, (f) $Ni_1B_{0.735}Mo_{0.025}$ treated at 500 °C for 2 hr.

2 hr, Ni crystalline diffraction peaks appear in the XRD spectra of the two catalysts, meaning that the transformation of Ni_3B and Ni_2B phases to Ni crystalline phase occurs for $Ni_1B_{0.645}$ catalyst. Additionally, with the comparison of the two catalysts with and without Mo addition, both treated at 500 °C for 2 hr, it is found that the full-width at half-maximum (FWHM) of the main diffraction peak of the later is smaller than that of the former, according to the equation of SCHERRER, indicating the crystalline grain size of the later is bigger than that of the former. This phenomenon might be also attributed to the dispersing effect of Mo, preventing the gathering of the Ni atoms, resulting in small crystalline grain size. Coupled with the analysis of DSC, it is reasonable to infer that Mo dopant first prevents the gathering of the Ni atoms, thus resulting in the shift of the first peak in DSC spectra to higher temperature and presenting smaller crystalline grain size observed in the XRD spectra, and then, from the viewpoint of Physical Chemistry Theory, the small crystalline grain size is prone to atomic diffusion and growing up [15] than the large one in that the second crystallization peak in DSC spectra shift to lower temperature.

Fig. 4 shows the H_2-TPD spectra of the Ni–B catalysts with and without Mo dopant. It is found that under lower Mo contents (atomic ratio of Mo to Ni < 0.025) there are two peaks (α and β), indicating two adsorbing sites, on the surface of the samples; while under higher Mo contents (≥ 0.025), only one peak (β') exists on the surface. With the increase of the Mo contents, the peak α shifts to higher temperatures, while the peak β shifts to lower temperatures; finally, the two peaks overlap with only one peak β' around 320 °C, implying that the surface of Ni–B amorphous alloy becomes homogeneous with the addition of Mo, further clarifying the existence of the dispersing effect of Mo.

Fig. 4 further shows that the total H_2-TPD area first increased and then decreased with the increase in the Mo contents. The biggest total area of H_2-TPD peaks was obtained when Mo contents was 0.025, following the same trend as the amounts of H_2-chemisorption.

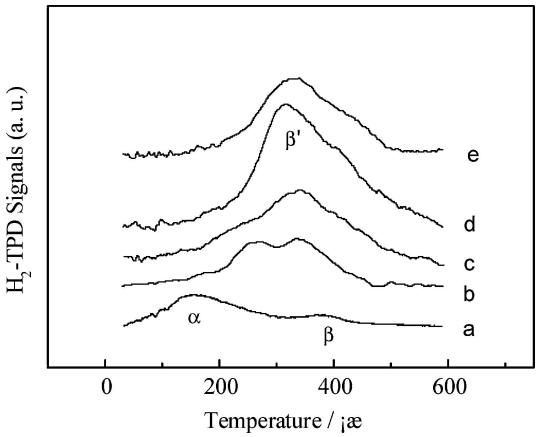

Figure 4 H_2-TPD spectra of the series of Mo-doped Ni–B amorphous alloy: (a) $Ni_1B_{0.645}$, (b) $Ni_1B_{0.667}Mo_{0.014}$, (c) $Ni_1B_{0.685}Mo_{0.020}$, (d) $Ni_1B_{0.735}Mo_{0.025}$, (e) $Ni_1B_{0.757}Mo_{0.034}$.

Thus, the H_2-TPD results further indicate that Mo species might disperse the surface active Ni atoms, resulting in more hydrogen adsorbed. However, too much Mo species might cover the surface Ni atoms, resulting in less hydrogen being adsorbed.

The catalytic activities of the various catalysts in the hydrogenation of EAQ are also given in Table I. It is found that the activities of Ni–B amorphous alloys catalysts are much higher than those of the crystallized $Ni_1B_{0.735}Mo_{0.025}$ catalysts. The activity first increased with the increase of Mo contents. As the atomic ratio of Mo to Ni is 0.025, the activity reached the maximum, 6.9×10^{-3} $g_{H_2O_2}$ g_{cat}^{-1} min^{-1}, which is higher than that of Raney Ni, i.e., 3.7×10^{-3} $g_{H_2O_2}$ g_{cat}^{-1} min^{-1} under the same reaction conditions [17]. However, further increase of Mo contents led to the decrease of the activity. This trend agreed with the results of H_2-TPD and H_2-chemisorption. The reaction kinetics of 2-ethylanthraquinone hydrogenation catalyzed by nickel catalysts had been determined to be first-order to hydrogen and zero-order to 2-ethylanthraquinone [18]. Thus, the main factor affected the catalytic activity would be the amounts of hydrogen adsorption. According to the earlier analysis, the higher activities of Ni–B amorphous catalysts than those of the crystallized samples might be attributed to, on one hand, to more hydrogen being adsorbed and on the other, the amorphous structure which has been proved to be favorable for the reactions of hydrogenation [19, 20]. With respect to the effects of Mo dopant on the activity of Ni–B amorphous alloy, it could be attributed to the dispersing effect of Mo, leading to more surface active Ni atoms; however, overmuch Mo might result in the coverage of surface Ni atoms.

Additionally, according to our previous research [17], the strong adsorbed hydrogen, desorbed around 300–400 °C in H_2-TPD, might be suitable for the hydrogenation of 2-ethlyanthraquinone. Therefore, with the Mo species addition, the shift of β desorption peak to lower temperatures in the spectra of H_2-TPD imply that the adsorbed hydrogen suitable to the hydrogenation was further activated, which is of advantage to the hydrogenation.

In summary, a series of Mo-doped Ni–B amorphous catalysts were prepared by KBH_4 reduction method,

and evaluated in the hydrogenation of EAQ. The roles of Mo dopant were found to be both strengthening the thermal stability and increasing the activity of Ni–B amorphous alloy used in 2-ethlyanthraquinone hydrogenation. All these effects might be attributed to the structural effects of Mo dopant, which improve the thermal stability, effectively disperse the surface Ni atoms, increase the amounts of hydrogen adsorbed and thereby enhance the catalytic activity. However, overmuch Mo addition might detrimentally cover some of the surface active Ni atoms, which eventually leads to lower activity.

Acknowledgments

This work has been supported by State Key Fundamental Research Project of China (Grant No. G2000048005) and National Natural Science Foundation of China (Grant No. 29873040).

References

1. G. SMITH, W. BROWER and MATYJASZCZYK, in Proceedings of 7th International Congress of Catalysis, Tokyo, 1980, edited by T. Seiyama and K. Tanabe (Elsevier, Amsterdam, 1981), p 355.
2. Y. CHEN, *Catal. Today* **44** (1998) 3.
3. H. LI, H. LI and J. F. DENG, *ibid.* **74** (2002) 53.
4. J. F. DENG, H. LI and W. WANG, *ibid.* **51** (1999) 113.
5. Y. HE, M. QIAO, H. HU, J. F. DENG and K. FAN, *Appl. Catal. A* **228** (2002) 29.
6. X. ZHANG, A. MA, X. MU and E. MIN, *Catal. Today* **74** (2002) 77.
7. J. F. DENG, *Curr. Top. Catal.* **2** (1999) 1.
8. R. ZHANG, F. LI, N. ZHANG and Q. SHI, *Appl. Catal. A* **239** (2003) 17.
9. Y. HOU, Y. WANG, L. WANG, Z. MI, W. WU and E. MIN, *J. Rare Earths* **22** (2004) 628.
10. Y. HOU, Y. WANG, F. HE, S. HAN, Z. MI, W. WU and E. MIN, *Mater. Lett.* **58** (2004) 1267.
11. B. ELVERS, S. HAWKINS, M. RAVENSCROFT and G. SCHULTZ, in "Encyclopedia of Industrial Chemistry," 5th Ed. (Wiley-VCH, Weinheim, 1989), p. 447.
12. Y. HOU, Y. WANG, F. HE, W. MI, Z. LI, Z. MI, W. WU and E. MIN, *Appl. Catal. A* **259** (2004) 35.
13. X. CHEN, H. LI, H. LUO and M. QIAO, *ibid.* **233** (2002) 13.
14. H. LI, H. LI and J. F. DENG, *Mater. Lett.* **50** (2001) 41.
15. J. L. WALTER, *Mater. Sci. Eng.* **50** (1981) 137.
16. N. ITOH, T. MACHIDA, W. C. XU, H. M. KIMURA and T. MASUMOTO, *Catal. Today* **25** (1995) 241.
17. Y. HOU, Y. WANG, S. HAN, Z. MI, W. WU and E. MIN, *Chin. J. Catal.* **25** (2004) 149.
18. T. BERGLIN and N. H. SCHÖÖN, *Ind. Eng. Chem. Process Des. Dev.* **20** (1981) 615.
19. M. SHIBATA and T. MASUMOTO, *Prep. Catal.* **4** (1987) 353.
20. A. MONLNAR, G. V. SMITH and M. BARTOK, *Adv. Catal.* **36** (1989) 329.

Received 20 December 2004
and accepted 25 July 2005